Figure S1

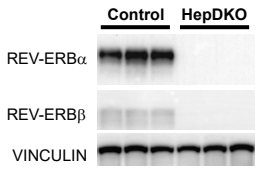

Figure S2

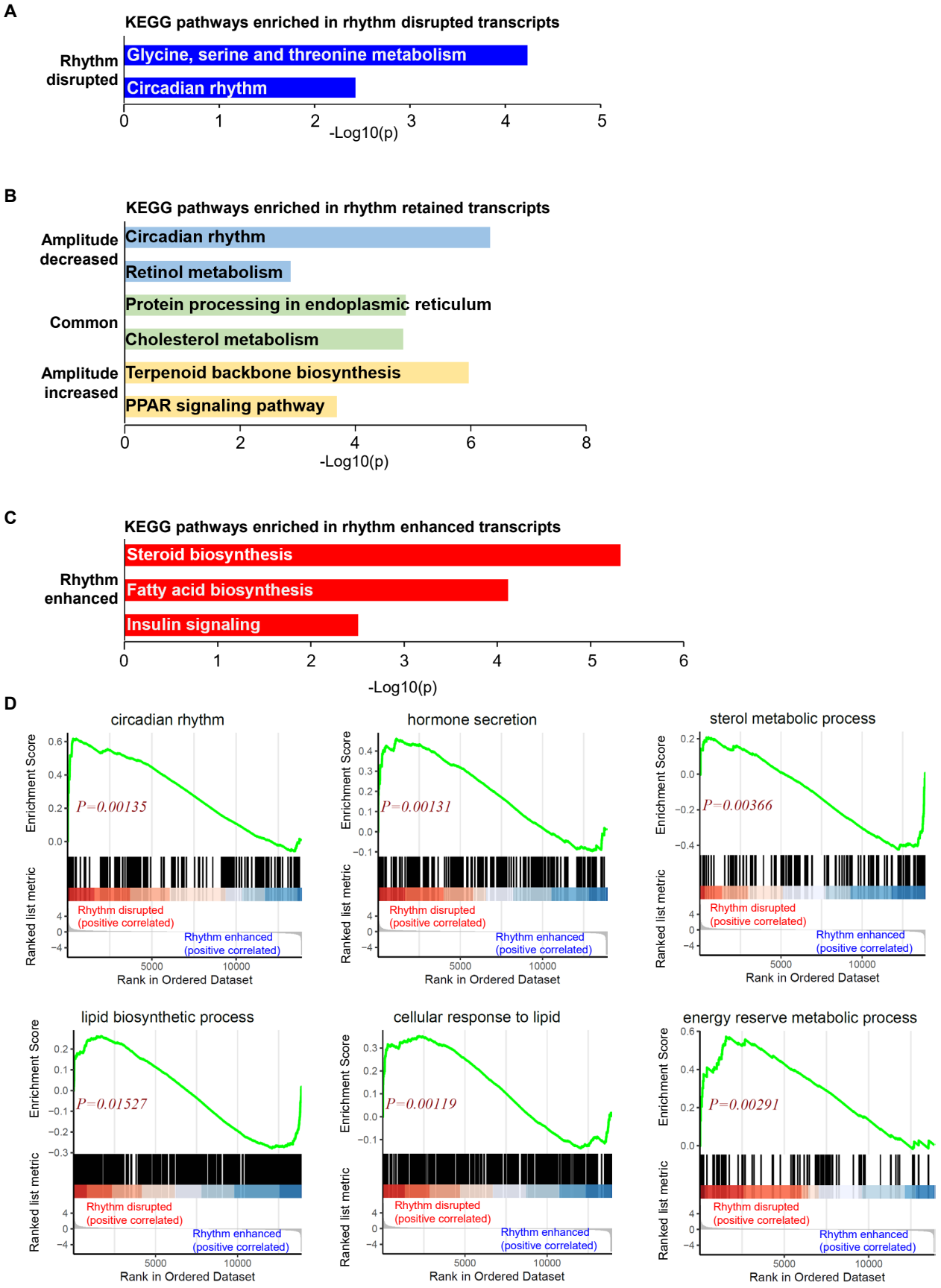
A
KEGG pathways enriched in rhythm disrupted transcripts
Rhythm disrupted
Glycine, serine and threonine metabolism
Circadian rhythm
0
1
2
3
4
5
-Log10(p)
B
KEGG pathways enriched in rhythm retained transcripts
Amplitude decreased
Circadian rhythm
Retinol metabolism
Common
Protein processing in endoplasmic reticulum
Cholesterol metabolism
Amplitude increased
Terpenoid backbone biosynthesis
PPAR signaling pathway
0
2
4
6
8
-Log10(p)
C
KEGG pathways enriched in rhythm enhanced transcripts
Rhythm enhanced
Steroid biosynthesis
Fatty acid biosynthesis
Insulin signaling
0
1
2
3
4
5
6
-Log10(p)
D
circadian rhythm
P=0.00135
hormone secretion
P=0.00131
sterol metabolic process
P=0.00366
lipid biosynthetic process
P=0.01527
cellular response to lipid
P=0.00119
energy reserve metabolic process
P=0.00291
Enrichment Score
Ranked list metric
Rhythm disrupted (positive correlated)
Rhythm enhanced (positive correlated)
Rank in Ordered Dataset
5000
10000

Figure S3

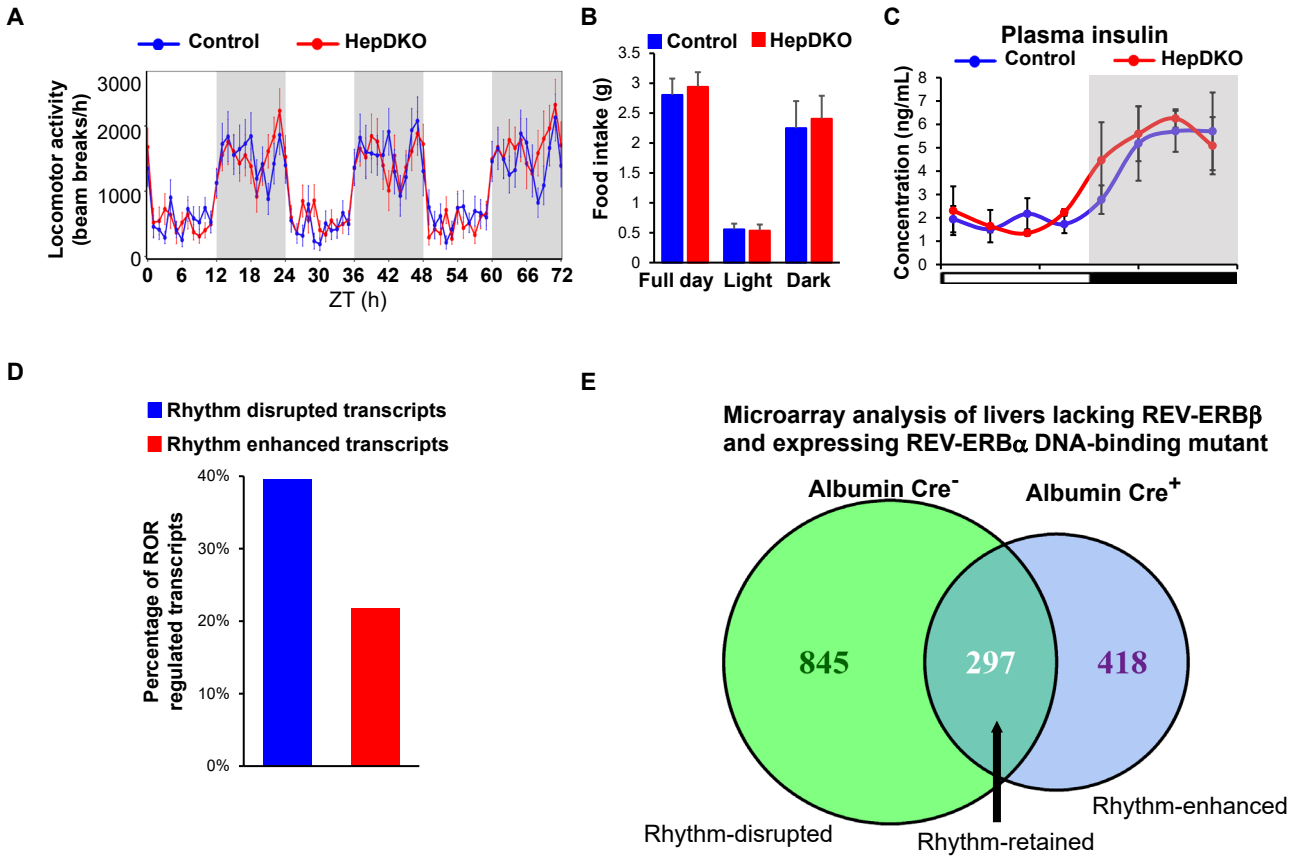
A
Control
HepDKO
Locomotor activity (beam breaks/h)
3000
2000
1000
0
0 6 12 18 24 30 36 42 48 54 60 66 72
ZT (h)
B
Control
HepDKO
Food intake (g)
3.5
3
2.5
2
1.5
1
0.5
0
Full day
Light
Dark
C
Plasma insulin
Control
HepDKO
Concentration (ng/mL)
8
7
6
5
4
3
2
1
0
D
Rhythm disrupted transcripts
Rhythm enhanced transcripts
Percentage of ROR regulated transcripts
40%
30%
20%
10%
0%
E
Microarray analysis of livers lacking REV-ERBβ and expressing REV-ERBα DNA-binding mutant
Albumin Cre-
Albumin Cre+
845
297
418
Rhythm-disrupted
Rhythm-retained
Rhythm-enhanced
F
Transcription factor binding enriched at rhythm retained transcripts
GIGGLE Score (Similarity)
250
200
150
100
50
0
BMAL1
PER2
CRY1
XBP1
TBP
CLOCK
ONECUT1
STAT5B
CREB1
PPARA
NR3C1
NCOR1
RXRA
ESR1
REV-ERBα
PER1
CRY2
HNF4A
ESRRA
FOXA1
Cistromes

Figure S4

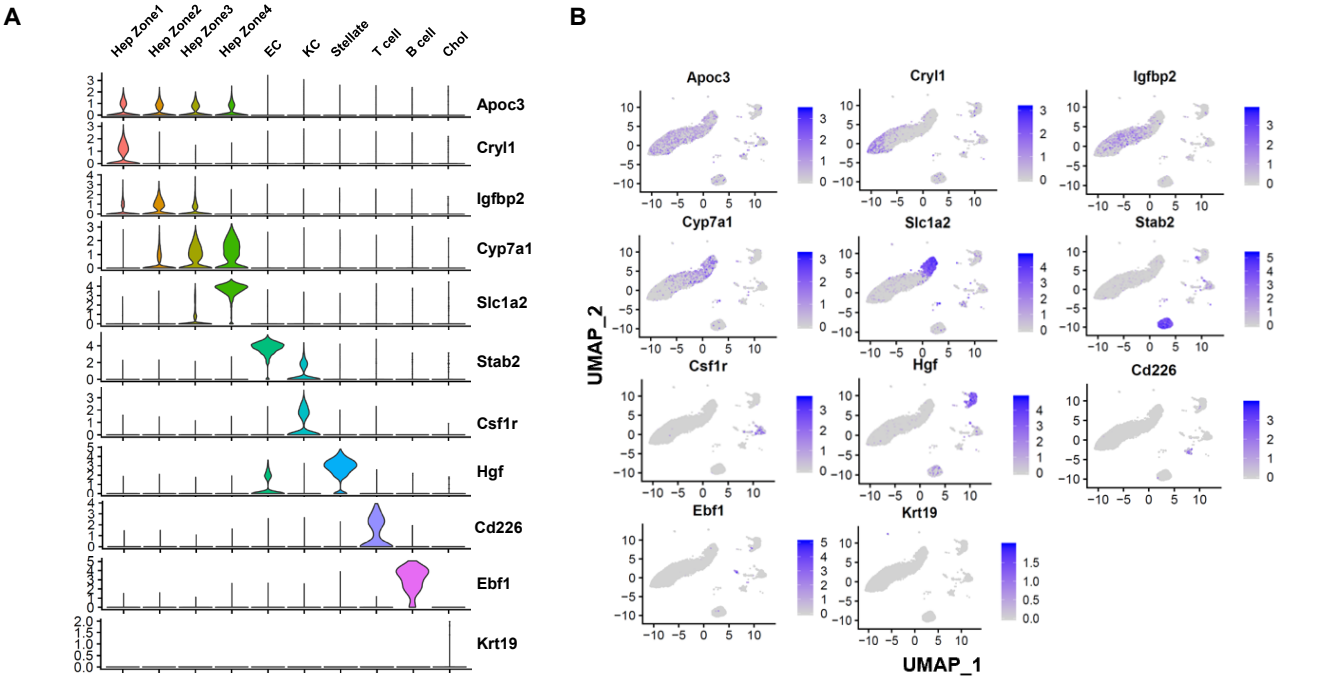

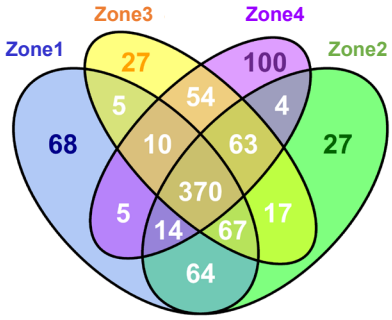

D

	Control	HepDKO
Total cell number	9171	9068
Hep Zone1	27.0%	30.7%
Hep Zone2	21.3%	24.2%
Hep Zone3	13.2%	11.9%
Hep Zone4	8.9%	9.0%
EC	12.7%	9.9%
Stellate	8.0%	6.7%
KC	5.9%	5.2%
T cell	1.9%	1.6%
B cell	0.7%	0.5%
Chol	0.4%	0.3%

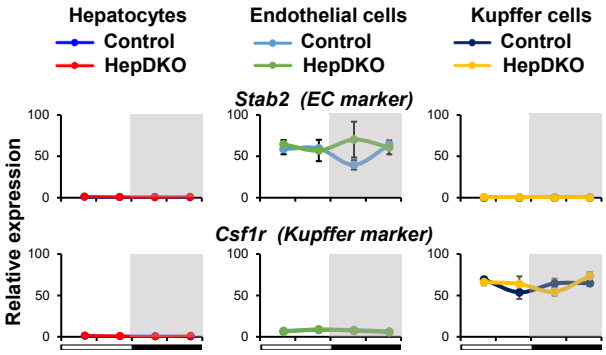

Figure S5

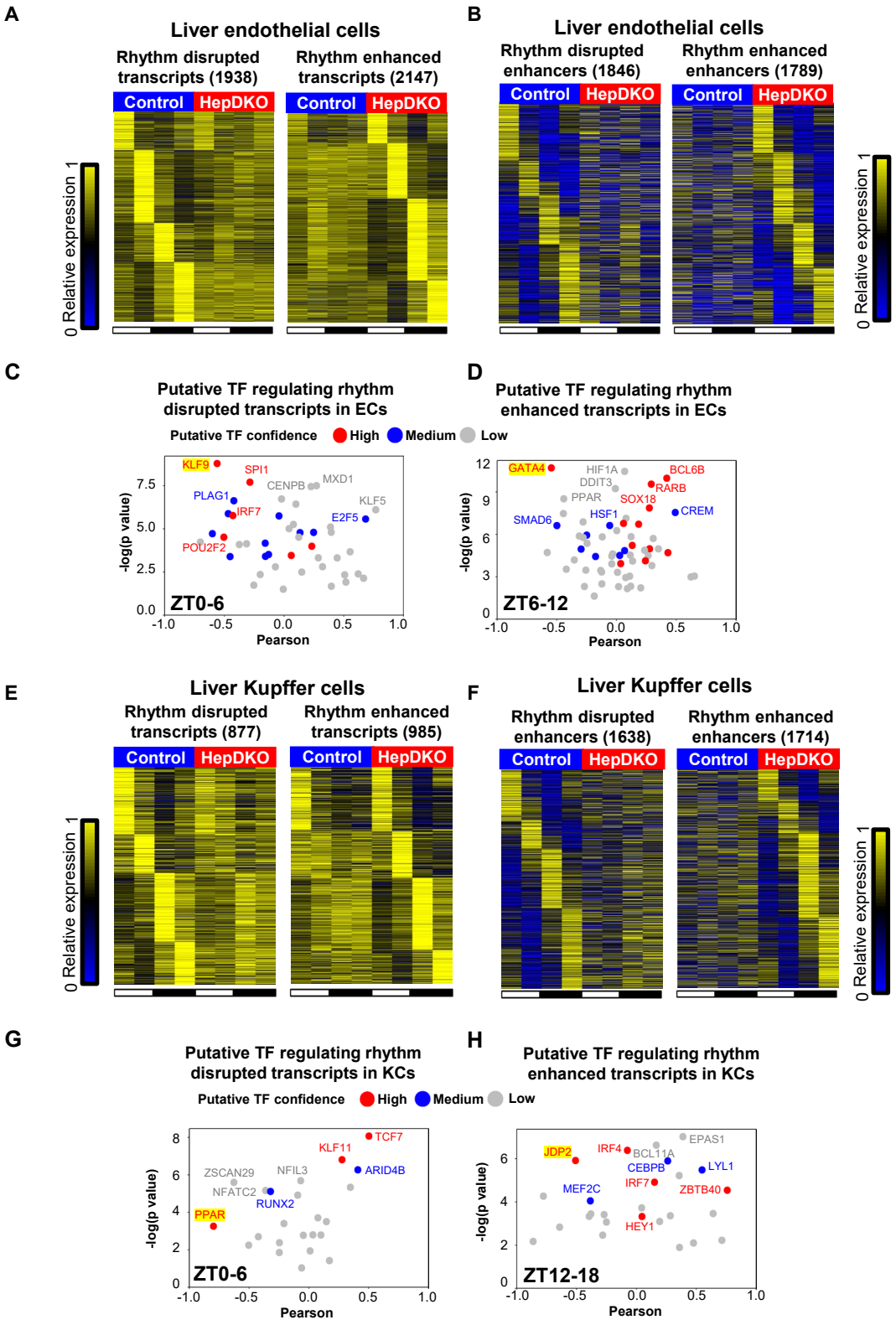
A
Liver endothelial cells
Rhythm disrupted transcripts (1938)
Rhythm enhanced transcripts (2147)
Control
HepDKO
0 Relative expression 1
B
Liver endothelial cells
Rhythm disrupted enhancers (1846)
Rhythm enhanced enhancers (1789)
C
Putative TF regulating rhythm disrupted transcripts in ECs
Putative TF confidence High Medium Low
KLF9
SPI1
CENPB
MXD1
PLAG1
IRF7
KLF5
E2F5
POU2F2
ZT0-6
-log(p value)
Pearson
D
Putative TF regulating rhythm enhanced transcripts in ECs
GATA4
HIF1A
DDIT3
BCL6B
RARB
PPAR
SOX18
HSF1
CREM
SMAD6
ZT6-12
E
Liver Kupffer cells
Rhythm disrupted transcripts (877)
Rhythm enhanced transcripts (985)
F
Liver Kupffer cells
Rhythm disrupted enhancers (1638)
Rhythm enhanced enhancers (1714)
G
Putative TF regulating rhythm disrupted transcripts in KCs
TCF7
KLF11
ARID4B
ZSCAN29
NFIL3
NFATC2
RUNX2
PPAR
ZT0-6
H
Putative TF regulating rhythm enhanced transcripts in KCs
EPAS1
JDP2
IRF4
BCL11A
CEBPB
LYL1
IRF7
MEF2C
ZBTB40
HEY1
ZT12-18

Figure S6

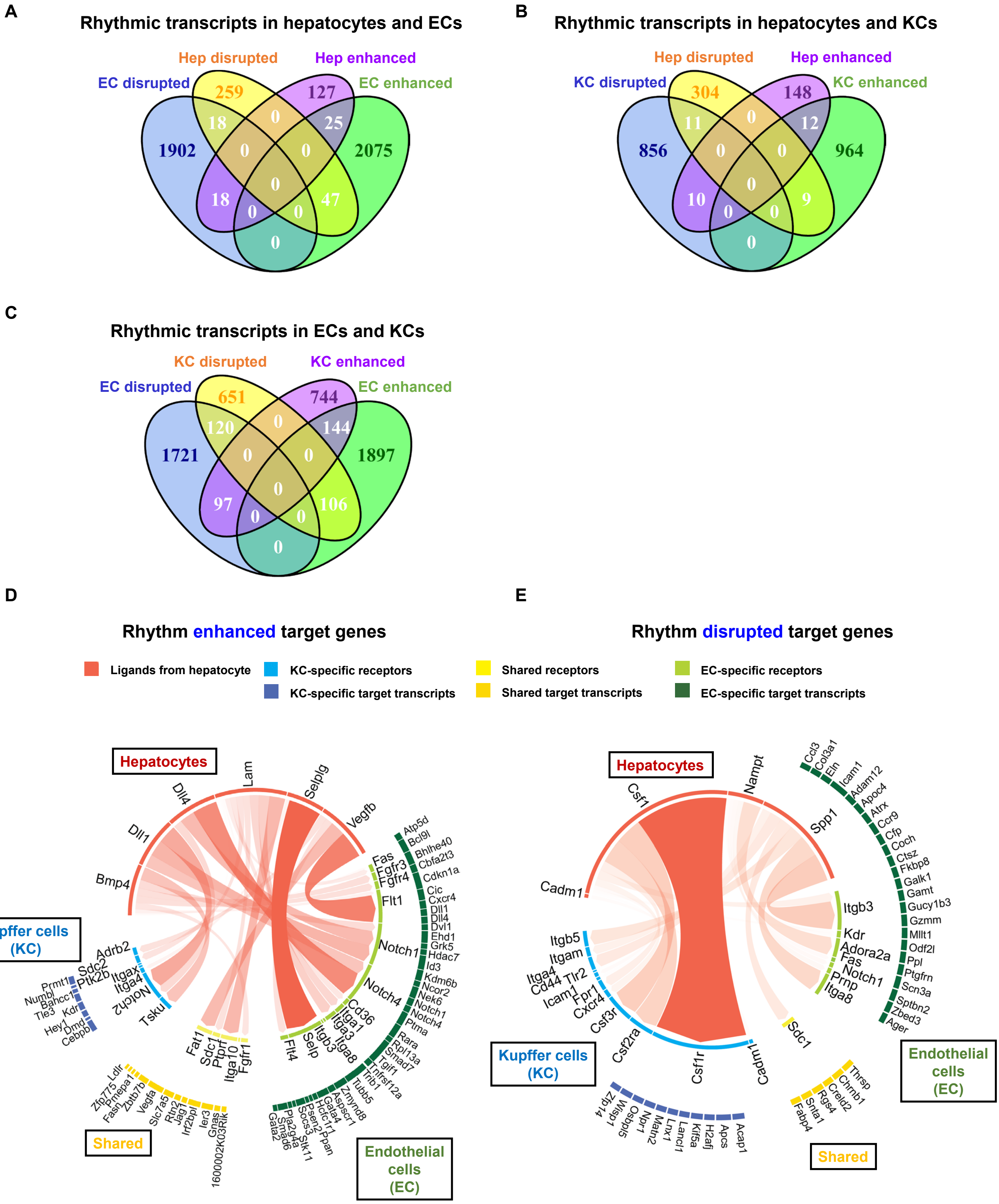
A
Rhythmic transcripts in hepatocytes and ECs
Hep disrupted
Hep enhanced
EC disrupted
EC enhanced
259
127
18
0
25
1902
0
0
2075
0
18
47
0
0
0
B
Rhythmic transcripts in hepatocytes and KCs
Hep disrupted
Hep enhanced
KC disrupted
KC enhanced
304
148
11
0
12
856
0
0
964
0
10
9
0
0
0
C
Rhythmic transcripts in ECs and KCs
KC disrupted
KC enhanced
EC disrupted
EC enhanced
651
744
120
0
144
1721
0
0
1897
0
97
106
0
0
0
D
Rhythm enhanced target genes
E
Rhythm disrupted target genes
Ligands from hepatocyte
KC-specific receptors
KC-specific target transcripts
Shared receptors
Shared target transcripts
EC-specific receptors
EC-specific target transcripts
Hepatocytes
Kupffer cells (KC)
Shared
Endothelial cells (EC)
Hepatocytes
Kupffer cells (KC)
Shared
Endothelial cells (EC)

Figure S7

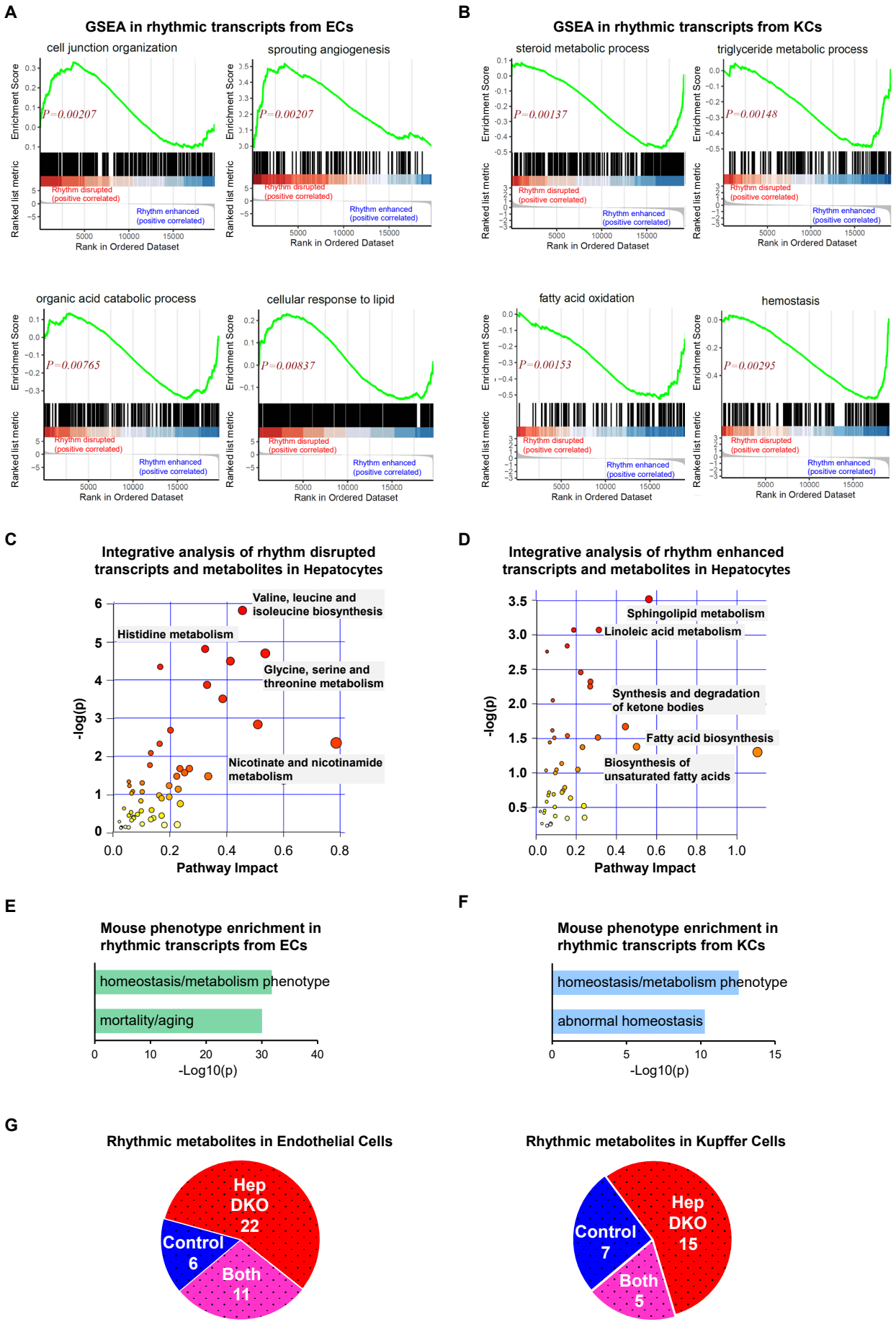
A
GSEA in rhythmic transcripts from ECs
cell junction organization
P=0.00207
sprouting angiogenesis
P=0.00207
organic acid catabolic process
P=0.00765
cellular response to lipid
P=0.00837
B
GSEA in rhythmic transcripts from KCs
steroid metabolic process
P=0.00137
triglyceride metabolic process
P=0.00148
fatty acid oxidation
P=0.00153
hemostasis
P=0.00295
Enrichment Score
Ranked list metric
Rhythm disrupted (positive correlated)
Rhythm enhanced (positive correlated)
Rank in Ordered Dataset
C
Integrative analysis of rhythm disrupted transcripts and metabolites in Hepatocytes
Valine, leucine and isoleucine biosynthesis
Histidine metabolism
Glycine, serine and threonine metabolism
Nicotinate and nicotinamide metabolism
-log(p)
Pathway Impact
D
Integrative analysis of rhythm enhanced transcripts and metabolites in Hepatocytes
Sphingolipid metabolism
Linoleic acid metabolism
Synthesis and degradation of ketone bodies
Fatty acid biosynthesis
Biosynthesis of unsaturated fatty acids
-log(p)
Pathway Impact
E
Mouse phenotype enrichment in rhythmic transcripts from ECs
homeostasis/metabolism phenotype
mortality/aging
-Log10(p)
F
Mouse phenotype enrichment in rhythmic transcripts from KCs
homeostasis/metabolism phenotype
abnormal homeostasis
-Log10(p)
G
Rhythmic metabolites in Endothelial Cells
Hep DKO 22
Control 6
Both 11
Rhythmic metabolites in Kupffer Cells
Hep DKO 15
Control 7
Both 5

Figure S8

Glutathione metabolism

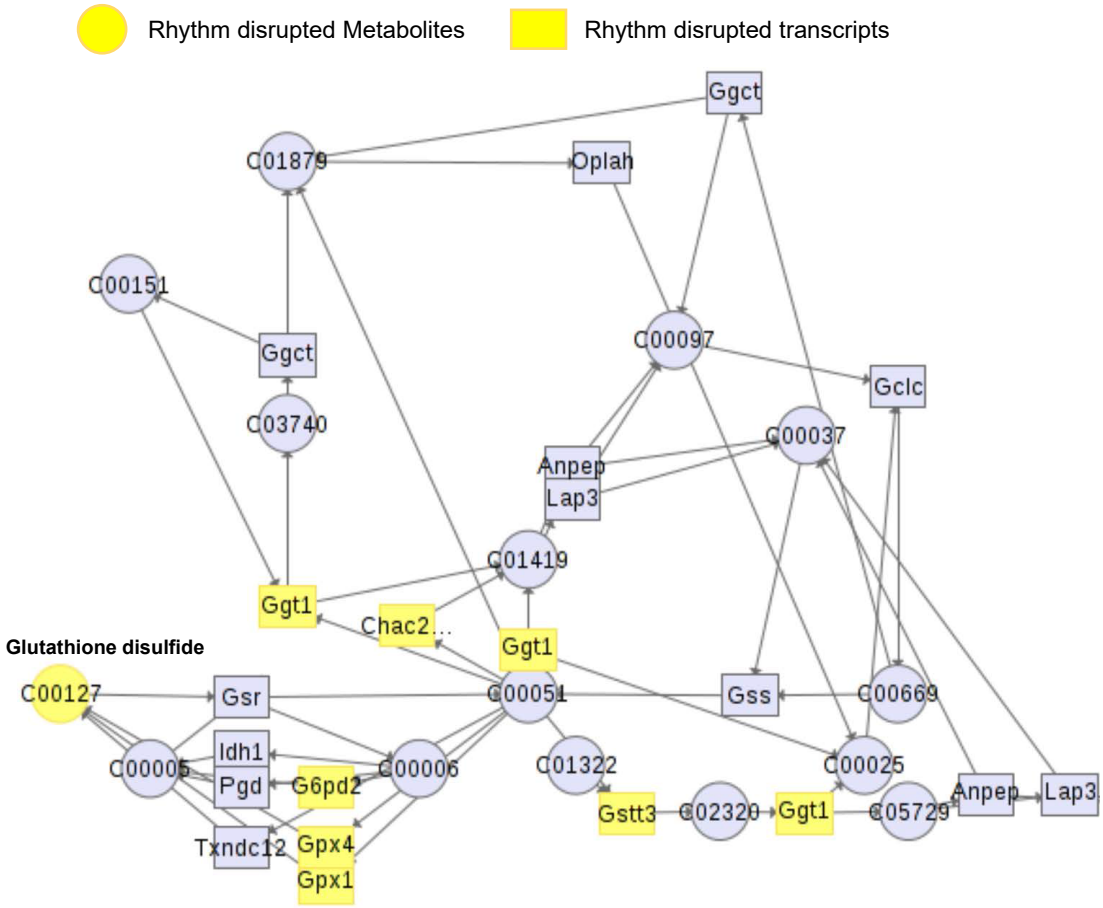

Figure S9

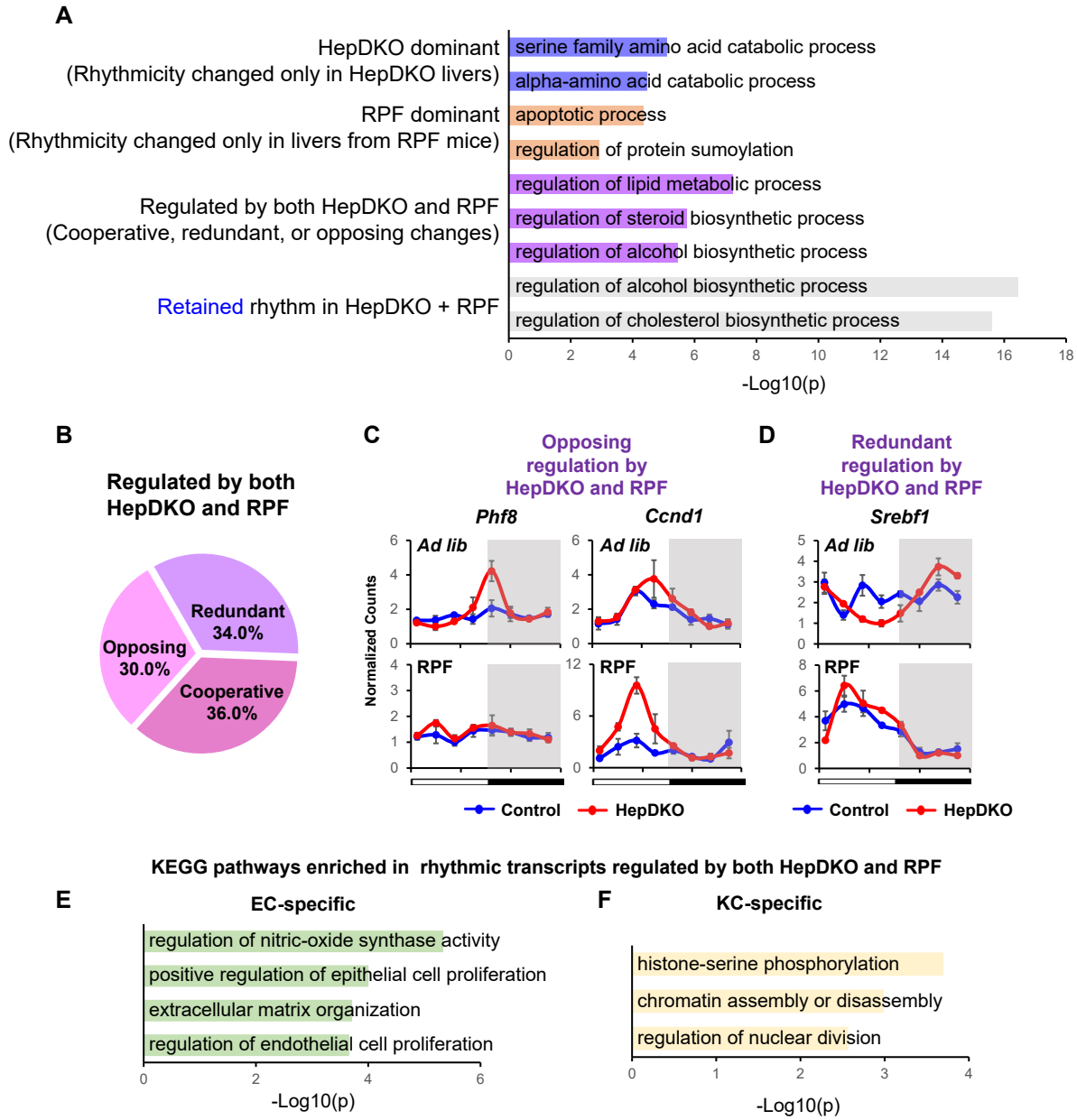
A
HepDKO dominant
(Rhythmicity changed only in HepDKO livers)
RPF dominant
(Rhythmicity changed only in livers from RPF mice)
Regulated by both HepDKO and RPF
(Cooperative, redundant, or opposing changes)
Retained rhythm in HepDKO + RPF
serine family amino acid catabolic process
alpha-amino acid catabolic process
apoptotic process
regulation of protein sumoylation
regulation of lipid metabolic process
regulation of steroid biosynthetic process
regulation of alcohol biosynthetic process
regulation of alcohol biosynthetic process
regulation of cholesterol biosynthetic process
0 2 4 6 8 10 12 14 16 18
-Log10(p)
B
Regulated by both HepDKO and RPF
Redundant 34.0%
Opposing 30.0%
Cooperative 36.0%
C
Opposing regulation by HepDKO and RPF
Phf8
Ccnd1
Ad lib
RPF
Normalized Counts
Control
HepDKO
D
Redundant regulation by HepDKO and RPF
Srebf1
Ad lib
RPF
Control
HepDKO
KEGG pathways enriched in rhythmic transcripts regulated by both HepDKO and RPF
E
EC-specific
regulation of nitric-oxide synthase activity
positive regulation of epithelial cell proliferation
extracellular matrix organization
regulation of endothelial cell proliferation
0 2 4 6
-Log10(p)
F
KC-specific
histone-serine phosphorylation
chromatin assembly or disassembly
regulation of nuclear division
0 1 2 3 4
-Log10(p)

Figure S10

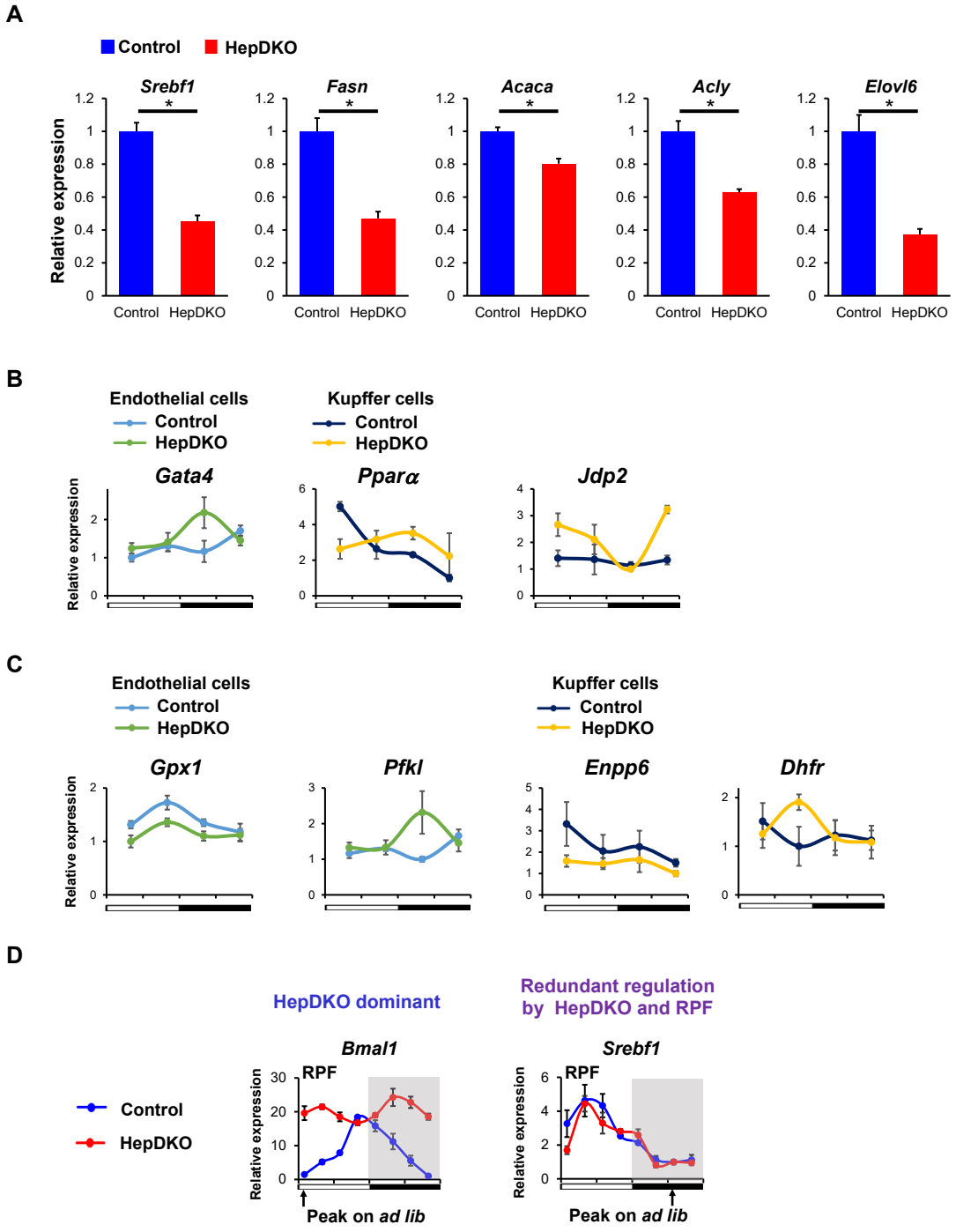
A
Control
HepDKO
Srebf1
Fasn
Acaca
Acly
Elovl6
Relative expression
Control
HepDKO
B
Endothelial cells
Kupffer cells
Control
HepDKO
Gata4
Pparα
Jdp2
Relative expression
C
Endothelial cells
Kupffer cells
Control
HepDKO
Gpx1
Pfkl
Enpp6
Dhfr
Relative expression
D
Control
HepDKO
HepDKO dominant
Redundant regulation
by HepDKO and RPF
Bmal1
Srebf1
RPF
Relative expression
Peak on ad lib
Peak on ad lib

Science
AAAS

Supplementary Materials for

The Hepatocyte Clock and Feeding Control Chronophysiology of Multiple Liver Cell Types

Dongyin Guan[1,2], Ying Xiong[1,2], Trang Minh Trinh[1,2], Yang Xiao[1,2], Wenxiang Hu[1,2], Chunjie Jiang[1,2], Pieterjan Dierickx[1,2], Cholsoon Jang[3,4], Joshua D. Rabinowitz[3], Mitchell A. Lazar[1,2,5*]

*Correspondence: Mitchell A. Lazar, MD, PhD (lazar@pennmedicine.upenn.edu)

This PDF file includes:
Materials and Methods
References
Figs. S1 to S10
Captions for Tables S1 to S10

Other Supplementary Materials for this manuscript include the following:

Tables S1 to S10 (Excel files)

Materials and Methods

Animal studies

Rev-erbα fl/fl; *Rev-erbβ* fl/fl animals were generated by breeding the *Rev-erbα* fl/fl to *Rev-erbβ* fl/fl animals on C57BL/6 background (Institut Clinique de la Souris, Illkirch, France) (*48*). To specifically delete REV-ERB α/β in adult hepatocytes, adeno-associated viruses (AAV) encoding GFP or CRE driven by the hepatocyte-specific TBG promoter (AAV-TBG-GFP for control and AAV-TBG-CRE for knockout) were prepared by the UPenn Vector Core and were intravenously injected with 1.5 x 10^{11} genome copies (GC) per mouse at 8 weeks of age. All mice were housed under a 12 hrs light and 12 hrs dark cycle (lights on at 7 a.m. [zeitgeber time 0, ZT0] and lights off at 7 p.m. [ZT12]). Experiments were carried out on 8-12 weeks old male mice. For diet-induced obesity experiments, mice were given a rodent diet with high fat and sucrose diet (Research Diets, D12492) for 4 weeks after AAV-TBG-GFP or AAV-TBG-CRE injection. For the reverse phase restricted feeding (RPF) experiments, mice received food from 7 a.m. until 7 p.m. To determine REV-ERB target transcripts while minimizing batch effects, we collected livers, extracted RNA, and generated RNA-seq libraries at the same time. At each time point, we alternated the sacrifice of control and HDKO mice to further avoid bias. All animal care and use procedures followed the guidelines of the Institutional Animal Care and Use Committee of the University of Pennsylvania in accordance with the guidelines of the NIH.

RNA extraction and quantitative PCR

Total RNA was extracted from snap-frozen liver tissues using Trizol reagent followed by RNeasy Mini Kit. The RNA was reverse-transcribed using the High-

Capacity cDNA Reverse Transcription Kit. Quantitative PCR was performed with Power SYBR Green PCR Master Mix and a QuantStudio 6 Flex instrument (Applied Biosystems), and analysis was performed by the standard curve method. Transcript expression was normalized to the mRNA level of the housekeeping transcript *Arbp* and the minimum level of the transcript in samples. Error bar represents the standard error of the mean (SEM). The primer sequences are shown in **Table S10**.

Immunoblotting

Protein was extracted from snap-frozen liver tissues using RIPA buffer (20mM Tris-HCl, pH 7.5, 200mM NaCl, 1mM EDTA, 1% Triton X-100, 1mM dithiothreitol and 0.1% SDS) with cOmplete Protease Inhibitor Cocktail (Roche) and PhosSTOP (Roche). Then, 2X sample buffer was added and proceeded by sodium dodecyl sulfate-polyacrylamide gel electrophoresis (SDS-PAGE) and western blotting as previously described (*49*) using the following antibodies: anti-REV-ERBα (1:1,000, Abcam #ab174309), anti-REV-ERBβ (1:1,000, Santa Cruz #sc-398252), and anti-VINCULIN-HRP(1:5,000, CST #E18799).

Locomotor activity and food intake monitoring

Locomotor activity of single-housed mice was measured by monitoring consecutive beam breaks in an optical beam using Comprehensive Laboratory Animal Monitoring System (CLAMS, Columbus Instruments) metabolic cages. Food intake was monitored by the mass of food consumed in the food hopper of the CLAMS cages.

Metabolic profiling

For triglyceride measurements, livers were homogenized in lysis buffer (140mM NaCl, 50 mM Tris (pH 7.4), and 1% Triton X-100) using the TissueLyser with steel beads. Triglyceride concentration in the liver tissue lysates and serum was then measured using a Triglyceride Assay Kit (StanBio) following the manufacturer's protocol. Serum insulin concentration was measured using a commercial kit (Crystal Chem).

In vivo lipogenesis assay

Mice were provided with 30 μl/g body weight D_2O (with 0.9% NaCl) via intraperitoneal injection at ZT8 and ZT20. Serum was collected via tail prior to and six hours after the injection. Serum samples (5 μl) were incubated with 0.5 mL of 0.3 M KOH in 90% methanol at 80°C for 1 hr in a 2 mL glass vial. Then, formic acid (50 μl) was added for neutralization. The saponified fatty acids were extracted by adding 0.25 mL of hexane, vortexing, and transferring the top hexane layer to a new glass vial. Samples were then dried under a nitrogen gas stream and re-dissolved in 100 μl of 1:1 isopropanol:methanol for LC-MS analysis. Fatty acids were detected with a quadrupole-orbitrap mass spectrometer (Q Exactive, Thermo Fisher Scientific, San Jose, CA) operating in a negative ion mode. The LC separation was achieved on a C8 column using a gradient of solvent A (90:10 water:methanol with 1 mM ammonium acetate and 0.2% acetic acid) and solvent B (90:10 methanol:isopropanol with 1 mM ammonium acetate and 0.2% acetic acid). The gradient was 0 min, 25% B; 2 min, 25% B; 4 min, 65% B; 16 min, 100% B; 20 min, 100% B; 21min, 25% B;

22 min, 25% B; 25 min, 25% B. Flow rate was 150 µL/min. Injection volume was 5 µL, and column temperature was 25 °C. The MS scan range was m/z 200-600 with a resolution of 140,000 at m/z 200. The automatic gain control (AGC) target was 5 × 105. Data were analyzed using the MAVEN software. For tracer experiments, isotope labeling was corrected for natural 13C abundance (*50*).

Endothelial cell and Kupffer cell isolation

Mice were anesthetized, and the livers were perfused with perfusion media (HBSS without calcium and magnesium, 500 µM EGTA, and 50 µg/ml Heparin) through the portal vein and then digested with digestion media (HBSS with 1.37 mM calcium and magnesium, 5mg/ml collagenase, and 0.04 mg/ml trypsin inhibitor). Digested tissue was suspended with DMEM media, and the suspension was passed through a 100 µm nylon mesh filter (BD Falcon). Suspended tissue was centrifuged at 50 g for 3 min to pellet hepatocytes. The supernatant containing non-parenchymal cells was centrifuged at 400 g for 5 min. The pellets were resuspend using MACS buffer (phosphate-buffered saline pH 7.2, 0.5% BSA and 2 mM EDTA) and incubated with anti-CD146 microbeads (Miltenyi Biotec) for ECs or anti-F4/80 microbeads (Miltenyi Biotec) for KCs and purified via magnetic-activated cell sorting columns (MACS) as instructed in the manual. To minimize the potential enzymatic activities, the samples were maintained at 4 ° C in every step. The isolated cells were either directly lysed with Trizol reagent for RNA-extraction or snap-frozen using liquid nitrogen and stored at -80 C for subsequent metabolite extraction and analysis.

RNA-sequencing

Total RNA was extracted (see RNA extraction) from liver tissue or isolated ECs and KCs. 1 ug total RNA of purified DNase-treated total RNA from biological replicates was processed with a RiboZero Magnetic rRNA removal kit. The RNA libraries were prepared using a TruSeq Stranded Total RNA Library Prep kit (Illumina, 20020599) according to the manufacturer's protocol.

RNA-seq sequencing data processing

RNA-seq reads were aligned to the University of California, Santa Cruz (UCSC) mouse genome mm9 genome browser using STAR (*51*). The tag directories were established, and normalized read counts were measured with RefSeq transcripts using Homer (*52*). The vector of time-ordered read per kb per ten million reads (RPKTM) values for each feature was duplicated, and input to JTK_CYCLE (*53*) as a 16-time point (liver tissue samples) or 8-time point (EC and KC samples) to allow thorough identification of oscillation patterns starting at each different time point as previously described (*54*).

For transcription factor (TF) binding similarity screening analysis, the genomic coordinates of selected transcripts were extended 1000 bp at the transcription start site and end site to cover the promoter region. CistromeDB (*13*) was then applied to determine the similarity between these genomic coordinates and published cistromes. The cistromes from mouse liver tissue or hepatocytes were selected for downstream analysis.

For RNA-seq in livers from *ad libitum* and RPF mice, only those transcripts with maximum RPKTM value > 5 identified in 4 or more samples in 8-time points were selected for downstream analysis. Transcripts that met three criteria (peak/tough > 2, period between 21-24, and p value < 0.01), were defined as rhythmic; otherwise, others were considered not to be rhythmic. For RNA-seq in isolated ECs and KCs, only those transcripts with maximum RPKTM value > 5 identified in 2 or more samples in 4-time points were selected for the downstream analysis. Transcripts that met three criteria (peak/tough > 1.5, period between 21-24, and p value < 0.05) were considered to be rhythmic.

Gene Set Enrichment Analysis (GSEA)

To identify pathways enriched in hepatocyte REV-ERB-regulated transcriptomes, we utilized the global gene expression patterns (all expressed transcriptomes rather than selected rhythmic transcripts) under different conditions to generate a ranking metric based on the ratio of peak/trough amplitude between control and REV-ERB HepDKO. This ranking metric was input into the GSEA-Preranked algorithm. R package “clusterProfiler” (*55*) was used for statistical analysis and visualization of functional profiles for genes and gene clusters. FDR < 0.25 was used as cutoff based on guidelines for GSEA analysis:

(https://www.gsea-msigdb.org/gsea/doc/GSEAUserGuideFrame.html?Interpreting_GSEA).

Single nucleus sequencing

The nuclei isolation protocol was adapted from the GRO-seq protocol as previously described (*54*). In brief, mice were anesthetized, and the livers were perfused with perfusion media through the portal vein. Livers were subjected to Dounce homogenization in cold swelling buffer (10 mM Tris pH 7.5, 2 mM $MgCl_2$, 3 mM $CaCl_2$, 2 U/ml Superase-In). After centrifugation at 400 g, the nuclei were extracted using lysis buffer (swelling buffer with 10% glycerol and 1% Igepal). After washing once with lysis buffer, the nuclei were resuspended in chilled (4 °C) nuclei wash and resuspension buffer (1X PBS, 1.0% BSA, and 0.2 U/μl RNase Inhibitor) with a nuclei concentration of 1000 nuclei/ul. 10,000 nuclei were immediately proceeded with the 10X Genomics Chromium Single-Cell 3' according to the manufacturer's instructions. The libraries from control and HepDKO liver were constructed based on the 10X Genomics Chromium Single-Cell 3' manufacturer's instructions and sequenced by NextSeq 500.

Single nuclei sequencing data analysis

Cell Ranger (3.0.2) software (10x Genomics) was run on the raw data using mm10. Output from Cell Ranger was loaded into R package Seurat (version 3.0) (*56*). After removing doublets and nuclei with low quality, 18,239 nuclei with more than 500 detected genes and less than 2% mitochondria genes were retained for further analysis. Unique sequencing reads for each gene were normalized to total Unique Molecular Identifiers (UMIs) in each nucleus to obtain normalized UMI values. Unsupervised clustering was applied after aligning the top 40 dimensions resulting from the PCA space using a resolution of 0.5. The identity for each cluster was assigned based on the prior knowledge of marker genes. The differential expressed genes in each cluster were defined

using a cutoff of $p < 0.01$ and fold change > 1.2. The UMAP plots, violin plots, Venn diagrams, and heat maps were generated by R.

Fast-ATAC sequencing

The process of fast-ATAC seq has been previously described (*57*). In brief, 50,000 isolated ECs or KCs were resuspended in 50 µl of transposase mixture (25 µl of 2X TD buffer, 2.5 µl of TDE1, 0.5 µl of 1% digitonin, and 22 µl of nuclease-free water) (15027865, Illumina). Transposition reactions were incubated at 37 °C for 30 min in an Eppendorf Thermo Mixer with agitation at 300 rpm. Transposed DNA was purified using a QIAGEN MinElute Reaction Cleanup kit (28204), and purified DNA was eluted in 10 µl of elution buffer (10 mM Tris-HCl, pH 8). Transposed fragments were amplified and purified as described previously (*58*). Libraries were quantified using KAPA Library Quantification Kits (Roche, KK4873). All Fast-ATAC libraries were sequenced using paired-end, dual-index sequencing on a NextSeq 500 instrument.

ATAC-seq data processing

The ATAC-seq analysis pipeline developed by Anshul Kundaje (Stanford University, Stanford, CA, USA) (https://github.com/kundajelab/atac_dnase_pipelines) was applied. For each sample, adapters were trimmed and aligned to the mouse genome mm9 with Bowtie. The aligned bam files of biological replicates were then merged and subjected to peak calling of open chromatin regions. The tag directories were established, and normalized read counts were measured using Homer (*52*).

Diurnal rhythmic enhancer identification

To identify diurnal rhythmic enhancers, we quantified intergenic eRNA expression as previously described (*21*). We first determined the intergenic enhancer region by filtering out those chromatin opening regions that overlapped with known coding regions and lncRNAs (with 1kb extension from both the transcription start site and transcription end site). Then, reads that mapped to ± 500 bp of the eRNA locus center were considered, and further normalized to RPKTM using Homer (*52*). Only those loci identified in 2 or more samples in ECs or KCs from control or HepDKO livers were selected for JTK_CYCLE analysis (*53*). Oscillating enhancers were defined as those with JTK_CYCLE adjusted $p \leq 0.05$, maximum RPKTM value > 0.2, oscillation amplitude (peak/trough) > 1.5, and oscillation period within the range of 21 to 24 hr.

Ligand receptor interaction analysis

To predict which ligands produced by hepatocytes regulate the rhythmicity remodeling in ECs and KCs, R package NicheNet (available at GitHub: https://github.com/saeyslab/nichenetr) (*27, 59*) was applied to rhythmic transcriptomes from whole liver tissue (most of the transcript expression signals from hepatocytes), isolated ECs and isolated KCs. The circle plots were generated via R package circlize (*60*). The impact of REV-ERB in hepatocytes on the expression of top predicated ligands was determined by the rhythmic transcriptome from liver tissues, and the expression of receptors was determined by the rhythmic transcriptome from ECs and KCs.

Metabolomics by LC-MS

Metabolites from snap-frozen isolated liver cell samples were extracted by adding -20°C methanol (100 µL per ~10^5 Kupffer cells or per ~10^6 endothelial cells), vortexing, and centrifuging at 16,000 x g for 10 min at 4°C. The supernatant was collected for LC-MS analysis. A quadrupole-orbitrap mass spectrometer (Q Exactive, Thermo Fisher Scientific, San Jose, CA) operating in negative or positive ion mode was coupled to hydrophilic interaction chromatography via electrospray ionization and used to scan from m/z 70 to 1000 at 1 Hz and 75,000 resolution. LC separation was performed on a XBridge BEH Amide column (2.1 mm x 150 mm, 2.5 µm particle size, 130 Å pore size; Waters, Milford, MA) using a gradient of solvent A (20 mM ammonium acetate, 20 mM ammonium hydroxide in 95:5 water:acetonitrile, pH 9.45) and solvent B (acetonitrile). Flow rate was 150 µL/min. The LC gradient was: 0 min, 85% B; 2 min, 85% B; 3 min, 80% B; 5 min, 80% B; 6 min, 75% B; 7 min, 75% B; 8 min, 70% B; 9 min, 70% B; 10 min, 50% B; 12 min, 50% B; 13 min, 25% B; 16 min, 25% B; 18 min, 0% B; 23 min, 0% B; 24 min, 85% B; 30 min, 85% B. The autosampler temperature was 5°C, and injection volume was 3 µL. Data were analyzed using the MAVEN software.

Diurnal rhythmic Metabolomics

After quantile normalization, the rhythmic metabolites were determined by JTK_CYCLE analysis (*53*). Oscillating metabolites were defined as those with JTK_CYCLE adjusted $p \leq 0.05$, oscillation amplitude (peak/trough) > 1.5, and oscillation period within the range of 21 to 24 hr. To integrate transcripts and metabolites for joint pathway analysis, MetaboAnalyst 4.0 (*31*) was applied

using adjusted $p < 0.01$ as the cutoff. Full list of metabolites can be found in **Table S7**.

Motif mining and IMAGE analysis

To identify TFs enriched in the loci of rhythmic enhancers, IMAGE analysis (*61*) was applied to integrate the signals both from rhythmic enhancers and transcripts. The motif mining was performed in each eRNA and transcript phase group using out-of-phase eRNAs and transcripts as background. Next, the transcription activity of identified motifs and mean expression of their putative target genes were determined. The phase-specific regulatory predicted TFs were selected by the following criteria: (1) the phase of TF transcription activity should match the phase of the mean expression of its putative target transcripts, and (2) the rhythmic expression pattern was validated in the rhythmic transcriptome from either ECs or KCs. Full list of predicted putative TFs can be found in **Table S4**.

EC-specific and KC-specific transcripts identification and rhythmic analysis

To determine EC-specific and KC-specific transcripts, the expressed transcripts were identified as RPKTM value > 1 based on RNA-seq data in hepatocytes, ECs, and KCs. The uniquely expressed transcripts in ECs and KCs were defined as EC-specific and KC-specific transcripts, respectively. Only those EC-specific and KC-specific transcripts with maximum RPKTM value > 1 identified in 2 or more samples of 4-time points in control or HepDKO livers from *ad libitum* and RPF mice were selected for the JKT_CYCLE analysis. Oscillating EC-specific and KC-specific transcripts were defined as those with

JTK_CYCLE adj.p ≤ 0.05, oscillation amplitude (peak/trough) > 1.5, and oscillation period within the range of 21 to 24 hr.

Data reproducibility and validation

The altered expression of lipid synthesis genes in control and HepDKO livers at ZT10, measured by RT-qPCR in Fig. 1H, was validated in an independent cohort of mice at ZT10 using RT-qPCR (**Fig. S10A**). Rhythmic expression of EC and KC transcripts that was calculated from RNA-seq data in Figs. 2K, 2P, and 2S was validated by RT-qPCR (**Fig. S10B)**. Rhythmic expression of EC and KC transcripts that was calculated from RNA-seq data in Figs. 3B, 3D, 3F, and 3H was validated by RT-qPCR (**Fig. S10C)**. Rhythmic transcript expression in RPF measured by RNA-seq for of *Bmal1* (Fig. 4D) and *Srebf1* (Fig. S9C) was validated by RT-qPCR (**Fig. S10D).**

Supplementary Figure Legends

Figure S1. REV-ERBα and β protein levels in control and HepDKO livers.

Figure S2. Pathway analysis of remodeled rhythmic transcripts. (**A-C**) KEGG pathways that were the most enriched ($p < 0.05$) in rhythm disrupted (**A**), retained (**B**) and enhanced (**C**) transcripts. (**D**) GSEA of remodeled rhythmic transcripts (FDR < 0.25).

Figure S3. Diurnal behavior and metabolism in HepDKO mice (**A-C**). Locomotor activity (**A**), food intake (**B**) and plasma insulin concentration (**C**) in control and HepDKO mice. **Comparison of HepDKO transcript expression with published datasets** (**D-F)**. (**D**) The overlap of rhythm disrupted and enhanced transcripts with genes in HepDKO liver with those reported to be regulated by RORα/γ in liver (*11*). (**E**) Analysis of microarray data from livers of mice in which Albumin-Cre (Alb-Cre+) was used to generate liver specific recombination that produced the REV-ERBα DNA-binding domain mutant and deleted REV-ERB (*12*). Rhythm disrupted, retained, and enhanced transcripts were characterized. (**F**) Rhythm retained transcripts in livers expressing REV-ERBα DNA-binding domain mutant and lacking REV-ERBβ were analyzed for TF binding similarity screening based on all published liver cistromes using CistromeDB (*13*).

Figure S4. Single nucleus sequencing (sNuc-Seq) analysis of livers from HepDKO and control mice. Hepatocyte REV-ERBs control non-hepatocytic

diurnal rhythmic transcriptomes. (**A**) Violin plots showing representative marker gene expression for each cluster in (**Fig. 2A**). (**B**) UMAP plots displaying the expression of representative marker genes. (**C**) Venn diagram of differentially expressed genes in hepatocytes from control and HepDKO livers. (**D**) Cell counts for hepatocyte zone1 (nearest to portal vein, Hep Zone1), hepatocyte zone2 (Hep Zone2), hepatocyte zone3 (Hep Zone3), hepatocyte zone4 (nearest to central vein, Hep Zone4), endothelial cells (EC), hepatic stellate cells (Stellate), Kupffer cells (KC), T cells, B cells, and Cholangiocytes (Chol). (**E**) Relative mRNA expression of *Stab2* (EC marker) and *Csf1r* (KC marker) in isolated hepatocytes, ECs and KCs from control and HepDKO livers.

Figure S5. Hepatocyte REV-ERBs control non-hepatocytic diurnal rhythmic transcriptomes. (**A and E**) Heat map of the relative expression of rhythm disrupted and enhanced transcripts in isolated ECs (**A**) and KCs (**E**) from control and HepDKO livers. (**B and F**) Heat map of the relative expression of rhythm disrupted and enhanced eRNAs in isolated ECs (**B**) and KCs (**F**) from control and HepDKO livers. The color bar indicates the scale used to show the expression of transcripts across eight time points, with the highest expression normalized to 1. JTK_CYCLE, adjusted $p < 0.05$, $21 \leq$ period (t) ≤ 24 hr, peak to trough ratio > 1.5 (n = 3 per time point). (**C, D, G and H**) - Log (p value) versus Pearson correlation plot for putative transcription factors identified by IMAGE for rhythm disrupted (**C**) and enhanced (**D**) transcripts in ECs, and rhythm disrupted (**G**) and enhanced (**H**) transcripts in KCs. Red = high-confidence factors, blue = medium-confidence factors, and gray = low-confidence factors.

Figure S6. Comparison of rhythm remodeled transcripts in hepatocytes, ECs and KCs upon REV-ERBs HepDKO. (A) Comparison of transcripts with whose rhythms were disrupted or enhanced by HepDKO in hepatocytes and ECs. (**B)** Comparison of transcripts with whose rhythms were disrupted or enhanced by HepDKO in hepatocytes and KCs. (**C)** Comparison of transcripts with whose rhythms were disrupted or enhanced by HepDKO in ECs and KCs. (**D and E**). **Ligand-receptor pair analysis.** Circle plots showing links between predicted ligands from hepatocytes (tomato) with their associated receptors from EC-specific (green), shared (yellow) and KC-specific (blue) associated rhythm enhanced (**D**) and disrupted (**E**) target transcripts potentially targeted by the ligand-receptors pairs.

Figure S7. Gene Set Enrichment Analysis (GSEA) of remodeled rhythmic transcripts in REV-ERBs HepDKO non-hepatic cells (A and B). (**A**) ECs. (**B**) KCs. FDR < 0.25. **Analysis of metabolite rhythms (C-F).** (**C and D**) Metabolic pathway analysis integrating the enrichment of genes and metabolites in rhythm disrupted (**C**) and enhanced (**D**) transcripts and metabolites in isolated hepatocytes. (**E and F**) Mouse phenotype enrichment in rhythmic transcripts from isolated ECs (**E**) and KCs (**F**) from control and HepDKO livers. (**G**) Identification of rhythmic metabolites in isolated ECs and KCs from control and HepDKO livers. JTK_CYCLE (Hughes et al., 2010), adjusted $p \leq 0.05$, $21 \leq$ period (t) ≤ 24 hr, peak to trough ratio > 1.5.

Figure S8. Disruption of glutathione metabolism in ECs from HepDKO livers. Integration of rhythm disrupted transcripts and metabolites in isolated ECs from control and HepDKO livers. Metabolites, circles; transcripts, rectangles. KEGG number is provided for specific metabolites.

Figure S9. Control of liver diurnal rhythms by the hepactocyte clock and feeding. (A) KEGG pathways most highly enriched ($p < 0.05$) in genes identified in Fig. 4E. **(B)** Pie chart related to Fig. 4E showing the proportion of cooperative, opposing, and redundant regulation among genes whose rhythmicity was regulated both by HepDKO and RPF. (**C and D**) Expression level (normalized read counts) of *Phf8*, *Ccnd1,* and *Srebf1* in control and HepDKO livers from *ad lib* and RPF mice. (**E and F**) KEGG pathways most highly enriched ($p < 0.05$) in rhythmic EC-specific transcripts (**E**) and KC-specific transcripts (**F**) regulated by both HepDKO and RPF.

Figure S10. Reproducibility and validation of gene expression data (**A**) Relative mRNA expression of *Srebf1* and its target genes in control and HepDKO livers collected at ZT10 (n = 4). (**B**) Relative mRNA expression of *Gata4* in isolated ECs, *Ppar*α and *Jdp2* in KCs isolated from control and HepDKO livers (n = 4). (**C**) Relative mRNA expression of *Gpx1* and *Pfkl* in isolated ECs, *Enpp6* and *Dhfr* in isolated KCs from control and HepDKO livers (n = 4). (**D**) Relative expression of *Bmal1* and *Srebf1* in control and HepDKO livers from RPF mice. Data are presented as mean ± SEM.

Supplementary Tables (tables published separately online in Excel format)

Table S1. Diurnal rhythmic transcripts identified by RNA-seq. Related to Figure 1.

Table S2. Cistrome data source for transcription factor binding similarity screening. Related to Figure 1.

Table S3. Diurnal rhythmic transcripts and eRNAs identified by RNA-seq and ATAC-seq in isolated Endothelial cells. Related to Figure 2.

Table S4. Putative factors with high or medium confidence responsible for rhythm disrupted and enhanced enhancers and transcripts. Related to Figure 2.

Table S5. Diurnal rhythmic transcripts and eRNAs identified by RNA-seq and ATAC-seq in isolated Kupffer cells. Related to Figure 2.

Table S6. Predicted ligands from hepatocytes and their associated receptors found in ECs and KCs by the ligand-receptors pairs. Related to Figure 2.

Table S7. JKT analysis of diurnal rhythmic metabolome. Related to Figure 3.

Table S8. Diurnal rhythmic transcripts identified by RNA-seq in *ad lib* feeding and RPF. Related to Figure 4.

Table S9. EC- and KC-specific diurnal rhythmic transcripts identified by RNA-seq in *ad lib* feeding and RPF. Related to Figure 4.

Table S10. Mouse qPCR primers used in this study. Related to Materials and Methods.